High harmonics generated in semiconductor nanostructures by the coupled dynamics of optical inter- and intraband excitations

D. Golde,[1] T. Meier,[2] and S. W. Koch[1]
[1]*Department of Physics and Material Sciences Center, Philipps University, Renthof 5, D-35032 Marburg, Germany*
[2]*Department Physik, Fakultät für Naturwissenschaften, Universität Paderborn, Warburger Strasse 100, D-33098 Paderborn, Germany*
(Received 10 October 2007; revised manuscript received 21 December 2007; published 27 February 2008)

The emitted radiation from semiconductor nanostructures due to the excitation with intense ultrashort optical laser pulses is analyzed. Semiconductor Bloch equations that consistently describe the coupled light-field-induced interband and intraband dynamics are solved numerically. It is demonstrated that the intraband dynamics considerably influences the light emission in the regime of extreme nonlinear optics. In particular, the intraband acceleration significantly modifies the dynamics of the interband polarization which results in a strong enhancement of high-harmonic generation.

DOI: 10.1103/PhysRevB.77.075330 PACS number(s): 42.65.Ky, 42.50.Hz, 78.47.−p

I. INTRODUCTION

The study of light-matter interactions with intense ultrafast laser pulses is a rapidly advancing research field yielding novel informations on fundamental light-matter interaction processes with significant application potential. Employing high-harmonic generation (HHG)[1,2] it became possible to initiate, observe, and control transient processes in atomic and molecular systems on attosecond time scales, see, e.g., Refs. 3–5. The fascinating regime of extreme nonlinear optics in which the Rabi frequency is comparable to or larger than the transition frequency can also be reached in semiconductors, see, e.g., Refs. 6. Interesting effects that have been predicted and observed in semiconductors include carrier-wave Rabi flopping,[7–9] HHG,[10–14] and the Mollow triplet.[15]

Theoretically the nonlinear optical response of two-level systems to intense ultrashort pulses has been studied by solving Bloch or Maxwell-Bloch equations.[7,10,11,14,16–18] In Refs. 12 and 19 the extreme nonlinear optical response of semiconductors with a continuous band structure has been modeled by an ensemble of inhomogeneously broadened two-level systems. The influence of the many-body Coulomb interaction among the photoexcited electrons and holes, which strongly influences the linear and nonlinear optical response of semiconductors in the regime where the light-matter interaction is not the dominating energy scale,[20,21] has been analyzed in a few investigations.[13,15,22] In Ref. 13 it has been shown that in two-dimensional semiconductor quantum wells and in one-dimensional semiconductor quantum wires the Coulomb interaction affects the light emission only weakly in the regime where the light-matter interaction dominates the energy scale. However, characteristic differences between the emission of a two-level system and extended semiconductors with a continuous dispersion have been demonstrated.[13]

Previous studies of the light emission of semiconductor nanostructures after excitation with intense femtosecond laser pulses have focused on light-field-induced interband transitions that give rise to carrier-wave Rabi flopping and HHG. Here, we extend the theoretical approach by additionally considering intraband excitations, i.e., the light-field-induced carrier acceleration. Such terms are well known to be relevant for descriptions of phototransport effects, e.g., optically detected Bloch oscillations[23] and dynamic localization[24] and the coherent generation of photocurrents by two-color excitation.[25–27] Here, a theory that consistently includes both interband and intraband excitations[23,24,26–28] is used to analyze the light emission of semiconductor nanostructures in the extreme nonlinear optical regime. Numerical solutions of the extended semiconductor Bloch equations (SBE) demonstrate that surprisingly the intraband acceleration strongly enhances the HHG compared to the case when only interband excitations are considered.

Our theoretical approach, i.e., SBE that describe the dynamics of the polarizations and the occupations due to interband and intraband excitation, is introduced in Sec. II. Numerical results on the emission in the regime of extreme nonlinear optics are presented and discussed in Sec. III. The intraband excitations lead to an additional radiation source via the light-field-induced current and also significantly modify the dynamics of the optical polarization. Altogether, the emission spectra are strongly enhanced towards high frequencies by the intraband acceleration. Furthermore, the influence of the band width and the effective mass on the emission is analyzed. Our most important results are summarized in Sec. IV.

II. THEORETICAL APPROACH

The coupled interband and intraband dynamics of semiconductor nanostructures is described by the SBE within a two-band model.[23,24,28] Since Ref. 13 showed no strong influence of the dimensionality on the light emission in the extreme nonlinear optical regime, we consider here a one-dimensional quantum wire and linearly polarized light fields, which allows us to ignore the vector character of the wave vector, the electric field, etc. Furthermore, we omit here the Coulomb interaction among the photoexcited carriers which influences the emission in the regime of extreme nonlinear optics only very weakly.[13] To understand this issue, one has to keep in mind that in semiconductors the Coulomb energy is typically of the order of the exciton binding energy. Thus, in extreme nonlinear optics, the energy scale describing the

light-matter interaction dominates the system response and the Coulomb interaction can in this case be regarded as a small perturbation. The equations of motion of the interband coherence (polarization) p_k and the occupation $n_k^{e(h)}$ of electrons (holes) read

$$i\hbar\frac{\partial}{\partial t}p_k = \left(\varepsilon_k^e + \varepsilon_k^h - i\frac{\hbar}{T_2}\right)p_k - (1 - n_k^e - n_k^h)d_k E(t) + ieE(t)\cdot\nabla_k p_k, \tag{1}$$

$$\hbar\frac{\partial}{\partial t}n_k^{e(h)} = -2\,\mathrm{Im}[d_k E(t)p_k^*] + eE(t)\cdot\nabla_k n_k^{e(h)}. \tag{2}$$

Here, $\varepsilon_k^{e(h)}$ are the single particle energies of the electrons (holes), T_2 is the dephasing time of the polarization, d_k is the (k-dependent) dipole matrix element, and $E(t)$ denotes the the electric field of the exciting laser pulse. While the terms proportional to $d_k E(t)$ in Eqs. (1) and (2) represent optical interband transitions, the intraband excitations are described by the terms proportional to $E(t)\cdot\nabla_k$. These terms lead to a time-dependent wave vector k which changes according to the acceleration theorem at a rate that is proportional to $E(t)$[29–31]

$$\frac{d}{dt}k(t) = -\frac{e}{\hbar}E(t). \tag{3}$$

In conventional optics, the rapidly oscillating changes of the wave vector that are induced by the optical fields are very small compared to typical wave vectors in a semiconductor. Therefore, the intraband dynamics usually does not modify the optical response significantly and consequently the intraband effects can often be neglected. In extreme nonlinear optics, however, the exciting fields are strong enough to cause very large transient shifts of the wave vector which can exceed the width of the Brillouin zone.[6] The results presented below demonstrate that in this regime the intraband effects cannot be neglected but play a major role for the optically-induced dynamics of the system and its emission.

Due to the motion of the carriers within the bands, a macroscopic current J arises which contributes to the light emission of the nanostructure in addition to the macroscopic polarization P. In the time domain these quantities are given by

$$P(t) = \sum_k [d_k p_k(t) + \text{c.c.}] \tag{4}$$

and

$$J(t) = \sum_{\lambda,k} e v_k^\lambda n_k^\lambda(t), \tag{5}$$

where d_k is the interband dipole matrix element, v_k^λ is the group velocity, i.e., proportional to the derivative of the dispersion with respect to k, and $\lambda = e, h$ is a band index. The time-dependent occupations $n_k^\lambda(t)$ and polarizations $p_k(t)$ which determine P and J are obtained by numerical solutions of the SBE, Eqs. (1) and (2).

The spectrum of the emitted radiation is given by

$$I_{\text{rad}}(\omega) \propto |\omega^2 P(\omega) + i\omega J(\omega)|^2. \tag{6}$$

Below, we distinguish between the total emission given by Eq. (6), the emission due to the interband polarization $I_{\text{rad}}^{\text{pol}} = |\omega^2 P(\omega)|^2$ and that due to the intraband current $I_{\text{rad}}^{\text{curr}} = |\omega J(\omega)|^2$. Eq. (6) shows that I_{rad} is not just given by the sum of the interband and intraband emission intensities, but also depends on the interference of $P(\omega)$ and $J(\omega)$. In addition to the numerical results that are presented and discussed in the following section, simplified analytical solutions of the SBE and of the polarization and current dynamics are provided in the Appendix.

III. NUMERICAL RESULTS

In order to keep the numerics as simple as possible, we consider a one-dimensional GaAs quantum wire in two-band approximation. However, as shown by our earlier comparisons,[13] the results presented should be qualitatively similar to those of quantum wells. The electron and heavy-hole dispersions are modeled as tight-binding bands that are proportional to $-\frac{\Delta_\lambda}{2}\cos(ka)$, where a is the lattice constant and Δ_λ is the width of band λ. If the curvature of the dispersion is chosen to coincide with that of a parabolic effective mass model, one has to use a band width that is inversely proportional to the effective mass m_λ[15,22,28]

$$\Delta_\lambda = \frac{2\hbar^2}{m_\lambda a^2}. \tag{7}$$

Using Γ-point effective masses of $m_e = 0.069 m_0$ and $m_{hh} = 0.5 m_0$ for the electron and heavy-hole bands, respectively, and the GaAs lattice constant of $a = 5.65$ Å results in band widths of $\Delta_e = 6.9$ eV for the conduction and $\Delta_h = 0.96$ eV for the valence band. In all calculations we consider an exciting laser pulse with Gaussian shape, a duration of $\tau = 10$ fs, and a central frequency that is resonant with the band gap, i.e., $E_G = \hbar\omega_0 = 1.43$ eV. The decay of the polarization is modeled by a dephasing time of $T_2 = 50$ fs.

Figure 1(a) shows the excitation dependent spectra if as in previous studies intraband excitations, i.e., the terms proportional to ∇_k in Eqs. (1) and (2) are neglected. In this case, the current J and thus $I_{\text{rad}}^{\text{curr}}(\omega)$ vanish and the total emission is due to the optical polarization, i.e., $I_{\text{rad}}(\omega) = I_{\text{rad}}^{\text{pol}}(\omega)$ and one obtains significant emission for frequencies $\omega \leqslant \alpha\omega_R$ with $\alpha \approx 2$. Incorporating the intraband acceleration into the theory strongly increases the width of the emission spectra, see Fig. 1(d), and the region of significant emission corresponds to $\alpha \approx 10$. Surprisingly, Figs. 1(b) and 1(c) show that the interband polarization $I_{\text{rad}}^{\text{pol}}$ and not the current $I_{\text{rad}}^{\text{curr}}$ is mainly responsible for the strong broadening of the emission spectra. It is thus the modification of the dynamics of the optical polarization $P(t)$ via the intraband acceleration that largely increases the HHG compared to calculations that consider only interband excitations. In the Appendix, this effect is analyzed qualitatively on the basis of simplified analytic investigations.

To analyze the different terms more precisely, the emission spectra for $\omega_R = 3\omega_0$ of the contour plot Fig. 1 are shown

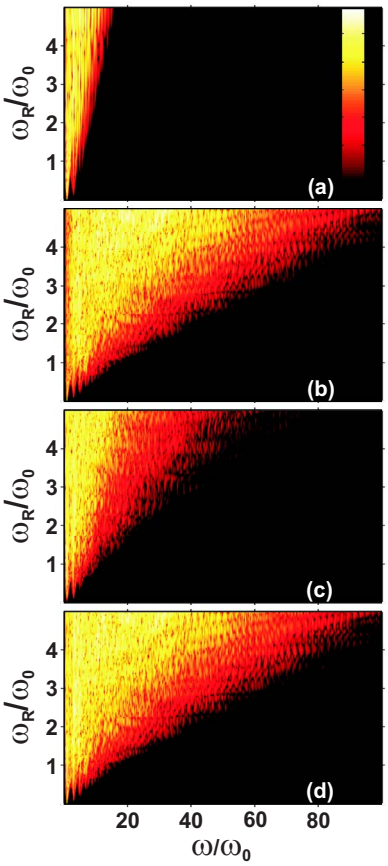

FIG. 1. (Color online) Excitation dependent emission of a GaAs quantum wire with a tight-binding band structure. ω is the spectrometer frequency, ω_R the peak Rabi frequency, and ω_0 the excitation frequency. The logarithmic color encoding covers seven orders of magnitude, see (a). In (a), the emission for pure interband dynamics is shown, i.e., $I_{\mathrm{rad}}(\omega)=I_{\mathrm{rad}}^{\mathrm{pol}}(\omega)$. (b), (c), and (d) show the spectra for coupled interband and intraband dynamics due to the polarization $I_{\mathrm{rad}}^{\mathrm{pol}}(\omega)$, the current $I_{\mathrm{rad}}^{\mathrm{curr}}(\omega)$, and the total emission $I_{\mathrm{rad}}(\omega)$, respectively.

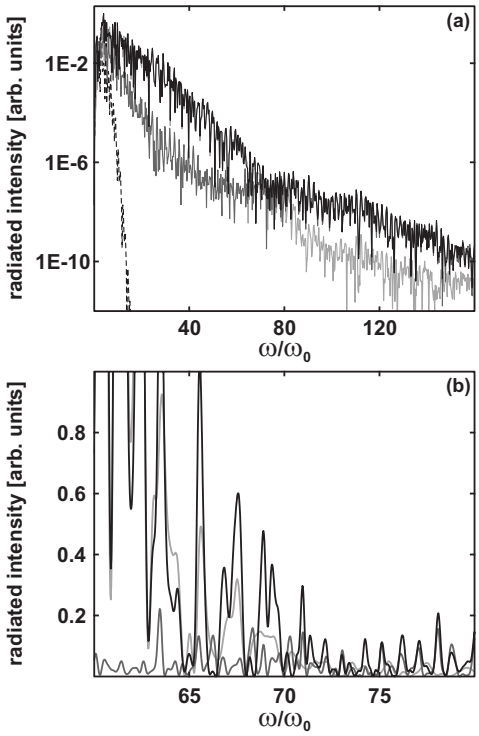

FIG. 2. Cross section through Fig. 1 at $\omega_R=3\omega_0$ for pure interband dynamics (dashed curve) and the coupled interband and intraband dynamics showing $I_{\mathrm{rad}}^{\mathrm{pol}}(\omega)$ (light gray curve), $I_{\mathrm{rad}}^{\mathrm{curr}}(\omega)$ (dark gray curve), and $I_{\mathrm{rad}}(\omega)$ (solid black curve). (a) The emission spectra on a logarithmic scale for a wide ω range, whereas in (b) the emission in the transition region, where $I_{\mathrm{rad}}^{\mathrm{pol}}(\omega)$ and $I_{\mathrm{rad}}^{\mathrm{curr}}(\omega)$ are comparable, is shown on a linear scale.

as lines in Fig. 2(a). For pure interband dynamics the emission intensity falls off rapidly with increasing frequency. When the coupled interband and intraband dynamics is considered, significant emission appears over a broader range and the decrease for large frequencies becomes much slower. The total emission intensity I_{rad} is basically given by the current-induced emission $I_{\mathrm{rad}}^{\mathrm{curr}}$ for $\omega \leqslant 60\omega_0$, whereas the polarization-induced emission $I_{\mathrm{rad}}^{\mathrm{pol}}$ dominates for $\omega \geqslant 80\omega_0$. Figure 2(b) shows I_{rad}, $I_{\mathrm{rad}}^{\mathrm{curr}}$, and $I_{\mathrm{rad}}^{\mathrm{pol}}$ in the transition region where the polarization- and the current-induced emission intensities are of comparable strength and interference effects are significant.

Clearly, the width of the conduction band $\Delta_e=6.9$ eV is unrealistic since such a wide conduction band would extend into the vacuum region where only unbound states exist. If one, however, reduces the bandwidth within the tight-binding model one, according to Eq. (7), simultaneously increases the effective mass. The total emission for a conduction band of width $\Delta_e=2.5$ eV which corresponds to a concomitant increase of the electron effective mass to $m_e=0.19m_0$ is shown in Fig. 3(a). Comparing to Fig. 1(d) demonstrates that the region of strong emission is smaller when the bandwidth is decreased.

To be able to vary bandwidth and effective mass separately, we use a model that includes nearest and second nearest neighbor interactions. In this case, the dispersion is pro-

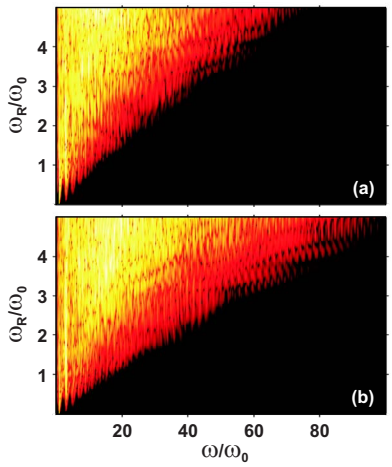

FIG. 3. (Color online) Total emission spectra $I_{\mathrm{rad}}(\omega)$ for coupled interband and intraband dynamics. In (a) a tight-binding model with a bandwidth of $\Delta_e=2.5$ eV and an effective mass of $m_e=0.19m_0$ is used. (b) is for a dispersion that includes also second-nearest neighbor interactions with $\Delta_e=2.5$ eV and $m_e=0.069m_0$.

portional to $A\cos(ka)+B\cos(2ka)$ and the two parameters A and B can be chosen to obtain the desired bandwidth and effective mass. In Fig. 3(b) we have evaluated such a model which has the same band width as in Fig. 3(a) of $\Delta_e = 2.5$ eV and the GaAs effective masses of $m_e = 0.069 m_0$. Comparing Figs. 3(a) and 3(b) demonstrates that for constant bandwidth the emission depends significantly on the effective mass or one could say on the details of the dispersion. In fact, the range of emission seen in Fig. 3(b) is not very different from that of Fig. 1(d), i.e., the width of the emission spectra depends much more strongly on the effective mass than on the band width. Alternatively, one can conclude that the maximum steepness of the band dispersion and not the bandwidth determines the broadness of the emission. This is understandable since for a steeper dispersion the intraband acceleration leads to a more rapid variation of the electron and hole energies $\varepsilon_k^{e/h}$ through the time-dependent wave vector. In order to obtain an improved physical understanding of this phenomenon, analytical solutions of Eqs. (1) and (2) for realistic excitation conditions are required which are presently not available.

IV. SUMMARY

The radiation emitted from a semiconductor quantum wire after extreme nonlinear optical excitation has been computed. Whereas most previous studies concentrate on interband excitations, we present and evaluate a theory that consistently describes the coupled light-field-induced interband and intraband dynamics. It is demonstrated that in the regime of extreme nonlinear optics the intraband acceleration significantly influences the light-field-induced dynamics and the emission. In particular, the intraband acceleration modifies the dynamics of the interband polarization. This results in a strongly enhanced generation of high harmonics as compared to the case when only interband excitations are considered.

ACKNOWLEDGMENTS

This work is supported by the Deutsche Forschungsgemeinschaft (DFG) and by the John von Neumann Institut für Computing (NIC), Forschungszentrum Jülich, Germany.

APPENDIX: SIMPLIFIED QUALITATIVE ANALYSIS

Already in the regime of ordinary nonlinear optics, i.e., for a Rabi frequency that is much smaller than the band gap, analytical solutions of the SBE, Eqs. (1) and (2), are only available for certain pulse shapes, e.g., ultrashort δ pulses or pulses with a constant envelope, for the cases of resonant or near-resonant excitation, which allows one to use the rotating-wave approximation to simplify the calculations.[20,21,28] When analyzing the generation of higher-harmonics in the regime of extreme nonlinear optics such simplifications are not possible[6,11,13] and consequently no analytical solutions for realistic pulse shapes are available.

In order to support our numerical findings, we therefore present in the following a number of simplified analytical results. We start with a two-level system whose polarization is given by

$$P(t) = d[p(t) + \text{c.c.}], \tag{A1}$$

which corresponds to Eq. (4) without the k summation. For excitation with an ultrashort pulse of the form

$$E(t) = \hat{E}(t)(e^{i\omega_0 t} + e^{-i\omega_0 t}), \tag{A2}$$

where $\hat{E}(t)$ is the envelope, we write the the time-dependent polarization as

$$P(t) = H(t)\Phi(t) = H(t)e^{i\varphi(t)}. \tag{A3}$$

Its Fourier transform is thus given by the convolution

$$P(\omega) = \int d\omega' H(\omega')\Phi(\omega - \omega'). \tag{A4}$$

During the excitation, $H(t)$ and $\Phi(t)$ are oscillating rapidly and due to coherent nonlinear dynamics of the two-level system, in particular, carrier-envelope Rabi flopping, this dynamics leads to the generation of higher harmonics $n\omega_0$ which are visible in the emission spectrum $I_{\text{rad}}^{\text{pol}}(\omega) = |\omega^2 P(\omega)|^2$.[6,11]

For the analysis of a two-band semiconductor, we incorporate the band dispersion into the equations given above and write

$$P(t) = \sum_k P_k(t) = \sum_k H_k(t)e^{i\varphi_k(t)} \tag{A5}$$

and

$$P(\omega) = \sum_k P_k(\omega) = \sum_k \int d\omega' H_k(\omega')\Phi_k(\omega - \omega'). \tag{A6}$$

Due to interferences among the complex $P_k(\omega)$'s which include resonantly and off-resonantly excited transitions, this inhomogeneous broadening modifies $I_{\text{rad}}^{\text{pol}}(\omega)$ compared to a two-level system.[13]

As discussed in Sec. II, the intraband acceleration that is described via the terms proportional to $ieE(t)\cdot\nabla_k$ in Eqs. (1) and (2), leads to a time-dependence of the wave vector $k(t)$ which varies with a rate that is proportional to the field amplitude $E(t)$. This means that the transition frequency $\omega_k^{eh} = (\varepsilon_k^e + \varepsilon_k^h)/\hbar$ becomes a function that through $k(t)$ acquires a rapid time dependence. For tight-binding dispersions we have

$$\omega_k^{eh}(t) = \omega_{\text{gap}} + \frac{\Delta_e + \Delta_h}{2\hbar}\{1 - \cos[k(t)a]\}. \tag{A7}$$

The time dependence of the wave vector is given by $k(t) = k_0 - \frac{e}{\hbar}\int_{-\infty}^{t} dt' E(t')$, i.e., for a constant field envelope $\hat{E}$, it oscillates as $\sin(\omega_0 t)$. Thus, in this case the explicit time evolution of the transition frequencies follows from

$$\omega_{k_0}^{eh}(t) = (\omega_{\text{gap}} + \omega_\Delta) - \omega_\Delta \cos\left(k_0 a + \frac{\omega_B}{\omega_0}\sin(\omega_0 t)\right)$$
$$= (\omega_{\text{gap}} + \omega_\Delta) - \omega_\Delta \cos(k_0 a)\cos\left(\frac{\omega_B}{\omega_0}\sin(\omega_0 t)\right)$$
$$- \omega_\Delta \sin(k_0 a)\sin\left(\frac{\omega_B}{\omega_0}\sin(\omega_0 t)\right) \tag{A8}$$

with $\omega_\Delta = \frac{\Delta_e + \Delta_h}{2\hbar}$ and the Bloch frequency $\omega_B = \frac{ea\hat{E}}{\hbar}$. In order to gain more insight into the actual temporal behavior of the transition frequencies, we rewrite the nontrivial contributions of Eq. (A8) as:

$$\cos\left(\frac{\omega_B}{\omega_0}\sin(\omega_0 t)\right) = \mathcal{J}_0\left(\frac{\omega_B}{\omega_0}\right) + 2\sum_{N=0}^{\infty}\mathcal{J}_{2N}\left(\frac{\omega_B}{\omega_0}\right)\cos(2N\omega_0 t) \tag{A9}$$

and

$$\sin\left(\frac{\omega_B}{\omega_0}\sin(\omega_0 t)\right) = 2\sum_{N=0}^{\infty}\mathcal{J}_{2N+1}\left(\frac{\omega_B}{\omega_0}\right)\cos[(2N+1)\omega_0 t], \tag{A10}$$

where $\mathcal{J}_N$ is the Nth order Bessel function of first kind. Obviously, the transition frequencies oscillate with multiple integers of the exciting field frequency ω_0. The intraband dynamics leads therefore, in particular, to an additional rapid oscillatory behavior of the phase $\varphi_k(t)$ that causes a broadening of $\Phi_k(\omega)$ and thus a broadening of $P(\omega)$ as compared to considering only interband excitations. This reasoning qualitatively explains the difference between Figs. 1(a) and 1(b), i.e., that the intraband excitations modify the interband dynamics and emission.

So far, we have dealt with the emission due to the polarization only. However, similar arguments explain the generation of higher harmonics in the emission due to the current $I_{\text{rad}}^{\text{curr}}(\omega)$. Surely, the current would vanish without intraband contributions since pure interband excitations create carrier occupations n_k^λ that are symmetric in k while the group velocity v_k^λ in Eq. (5) is an odd function of k.

The intraband motion leads to unsymmetric distribution functions and thus, to a finite current. For tight-binding bands, the group velocity is given by $v_k^\lambda = \frac{ea\Delta_\lambda}{2\hbar}\sin(ka)$. Inserting this into Eq. (5) and taking into account the time dependence of the wave vector for constant field envelopes yields

$$J(t) = -ea\omega_\Delta \sin\left(\frac{\omega_B}{\omega_0}\sin(\omega_0 t)\right)\sum_{k_0} n_{k_0}(t)\cos(k_0 a). \tag{A11}$$

Again, this expression can be expanded in terms of Bessel functions which unravels the high-harmonic oscillations

$$J(t) = -ea\omega_\Delta 2\sum_{N=0}^{\infty}\mathcal{J}_{2N+1}\left(\frac{\omega_B}{\omega_0}\right)\sin[(2N+1)\omega_0 t]$$
$$\times\sum_{k_0} n_{k_0}(t)\cos(k_0 a). \tag{A12}$$

The interband dynamics leads to a time dependence of $n_{k_0}(t)$ via carrier-wave Rabi flopping and thus, modifies the current in addition to the intraband contributions. Hence, the actual dynamics of the current, similarly to the polarization dynamics, results from a nontrivial coupling of interband and intraband excitations each producing high Fourier components that leads to the broad emission spectrum of Fig. 1(c).

The simplified analysis presented in this appendix qualitatively explains the high harmonic generation due to coupled interband and intraband dynamics. However, if one wants to obtain quantitative analytical results, e.g., unravel the relative importance of both contributions, see, e.g., Figs. 1 and 2, it is required to solve Eqs. (1) and (2) analytically for realistic pulse shapes and excitation conditions. Unfortunately, such solutions are not available.

[1] P. B. Corkum, Phys. Rev. Lett. **71**, 1994 (1993).
[2] M. Lewenstein, P. Balcou, M. Y. Ivanov, A. L'Huillier, and P. B. Corkum, Phys. Rev. A **49**, 2117 (1994).
[3] T. Brabec and F. Krausz, Rev. Mod. Phys. **72**, 545 (2000).
[4] *Few-Cycle Laser Pulse Generation and Its Applications*, edited by F. X. Kärtner, Vol. 95 of *Topics in Applied Physics* (Springer, Berlin, 2004).
[5] P. B. Corkum and F. Krausz, Nat. Phys. **3**, 381 (2007).
[6] M. Wegener, *Extreme Nonlinear Optics* (Springer, Berlin, 2005).
[7] S. Hughes, Phys. Rev. Lett. **81**, 3363 (1998).
[8] O. D. Mücke, T. Tritschler, M. Wegener, U. Morgner, and F. X. Kärtner, Phys. Rev. Lett. **87**, 057401 (2001).
[9] O. D. Mücke, T. Tritschler, and M. Wegener, in *Few-Cycle Laser Pulse Generation and Its Applications*, (Ref. 4), pp. 379–410.
[10] S. Hughes, Phys. Rev. A **62**, 055401 (2000).
[11] T. Tritschler, O. D. Mücke, and M. Wegener, Phys. Rev. A **68**, 033404 (2003).
[12] T. Tritschler, O. D. Mücke, M. Wegener, U. Morgner, and F. X. Kärtner, Phys. Rev. Lett. **90**, 217404 (2003).
[13] D. Golde, T. Meier, and S. W. Koch, J. Opt. Soc. Am. B **23**, 2559 (2006).
[14] C. Van Vlack and S. Hughes, Opt. Lett. **32**, 187 (2006).
[15] Q. T. Vu, H. Haug, O. D. Mücke, T. Tritschler, M. Wegener, G. Khitrova, and H. M. Gibbs, Phys. Rev. Lett. **92**, 217403 (2004).
[16] R. W. Ziolkowski, J. M. Arnold, and D. M. Gogny, Phys. Rev. A **52**, 3082 (1995).
[17] V. P. Kalosha and J. Herrmann, Phys. Rev. Lett. **83**, 544 (1999).
[18] X. Song, S. Gong, W. Yang, and Z. Xu, Phys. Rev. A **70**, 013817 (2004).
[19] O. D. Mücke, T. Tritschler, M. Wegener, U. Morgner, and F. X. Kärtner, Phys. Rev. Lett. **89**, 127401 (2002).
[20] H. Haug and S. W. Koch, *Quantum Theory of the Optical and Electronic Properties of Semiconductors*, 4th ed. (World Scientific, Singapore, 2004).

[21] W. Schäfer and M. Wegener, *Semiconductor Optics and Transport Phenomena* (Springer, Berlin, 2002).
[22] Q. T. Vu and H. Haug, Phys. Rev. B **71**, 035305 (2005).
[23] T. Meier, G. von Plessen, P. Thomas, and S. W. Koch, Phys. Rev. Lett. **73**, 902 (1994).
[24] T. Meier, F. Rossi, P. Thomas, and S. W. Koch, Phys. Rev. Lett. **75**, 2558 (1995).
[25] R. Atanasov, A. Haché, J. L. P. Hughes, H. M. van Driel, and J. E. Sipe, Phys. Rev. Lett. **76**, 1703 (1996).
[26] H. T. Duc, T. Meier, and S. W. Koch, Phys. Rev. Lett. **95**, 086606 (2005).
[27] H. T. Duc, Q. T. Vu, T. Meier, H. Haug, and S. W. Koch, Phys. Rev. B **74**, 165328 (2006).
[28] T. Meier, P. Thomas, and S. W. Koch, *Coherent Semiconductor Optics: From Basic Concepts to Nanostructure Applications* (Springer, Berlin, 2007).
[29] C. Kittel, *Quantum Theory of Solids* (Wiley, New York, 1963).
[30] A. Nenciu and G. Nenciu, Phys. Lett. **78A**, 101 (1980).
[31] J. B. Krieger and G. J. Iafrate, Phys. Rev. B **33**, 5494 (1986).